View metadata, citation and similar papers at core.ac.uk
brought to you by CORE
provided by RERO DOC Digital Library

Multibody System Dynamics (2005) 13: 447–463 © Springer 2005

Formulation and Preparation for Numerical Evaluation of Linear Complementarity Systems in Dynamics

CHRISTOPH GLOCKER and CHRISTIAN STUDER
IMES - Center of Mechanics, ETH Zurich, CH-8092 Zurich, Switzerland;
E-mail: christoph.glocker@imes.mavt.ethz.ch

(Received 4 February 2004; accepted in revised form 19 May, 2004)

Abstract. In this paper, we provide a full instruction on how to formulate and evaluate planar frictional contact problems in the spirit of non-smooth dynamics. By stating the equations of motion as an equality of measures, frictional contact reactions are taken into account by Lagrangian multipliers. Contact kinematics is formulated in terms of gap functions, and normal and tangential relative velocities. Associated frictional contact laws are stated as inclusions, incorporating impact behavior in form of Newtonian kinematic impacts. Based on this inequality formulation, a linear complementarity problem in standard form is presented, combined with Moreau's time stepping method for numerical integration. This approach has been applied to the woodpecker toy, of which a complete parameter list and numerical results are given in the paper.

Keywords: unilateral constraints, friction, impact, time stepping, linear complementary problem

1. Introduction

During the last years, increasing interest in the behavior of dynamic systems with discontinuities has been observed in nonlinear dynamics, comprising in particular friction and impact problems. As research in the past was primarily focussed on systems with a single non-smooth interaction element, current trends point towards more and more complex situations, involving combined frictional and unilateral impact behavior and multi-contact problems. The latter has been a topic of active research for years in the area of non-smooth mechanics, concerning e.g. the modeling and mathematical formulation of set-valued interaction laws via inclusions, existence and uniqueness results of the associated measure differential inclusions, as well as the development of numerical algorithms for solving both, inequality and evolution problems. This concise paper is intended to prepare some existing material in this field in a most comprehensive and condensed form, such that the interested reader should find a quick access to the methods used. Among many approaches, we have chosen the concept of linear complementarity to embed a subclass of non-smooth dynamic systems in mechanics, i.e. multibody systems with planar frictional impact contacts. We present a theoretical framework that is sufficiently wide to treat fully finite-dimensional dynamic systems with planar unilateral

Coulomb-contact constraints. A second goal is to show a general strategy on how to set up linear complementarity problems in a most efficient way when set-valued relay functions are involved. This step is non-trivial. In this paper, an LCP in standard form is formulated with closest possible connection to optimization theory and with a minimum of equations and operations for matrix inversion. An example that fits in with this class of problems is the woodpecker toy, which might serve as a benchmark problem for low-dimensional non-smooth systems. The paper is self-contained in the sense that everything needed to evaluate the woodpecker example, from the description of the model and a complete data list up to the numerical results obtained by the presented time stepping method, is included.

The paper is organized as follows: In Section 2 we introduce the two most basic set-valued maps defined on $\mathbb{R}$, the unilateral primitive $\mathrm{Upr}(x)$ and the filled-in relay function $\mathrm{Sgn}\,(x)$. It is shown that the relay function can be decomposed into two unilateral primitives, which is later quintessential when the linear complementarity problem of the dynamic system with planar frictional contacts is formulated. The theoretical framework for the formulation of a frictional contact problem in finite freedom dynamics is briefly presented in Section 3. We follow exactly the work in [12], but narrow it already down to planar unilateral Coulomb contacts with Newtonian impacts to have later access to linear complementarity. We give a complete formulation of the dynamic process based on a measure differential inclusion and try to clearly arrange the full set of unilateral contact-impact laws. The woodpecker in Section 4 serves as a typical example for a low-dimensional dynamic system with frictional unilateral contacts. The full model is presented, together with a complete list of parameters that have been used for the numerical simulation. As results, we show the time history of the angular displacements and velocities of the woodpecker body and sleeve, and the associated limit cycles in the phase space. Section 5 reviews the midpoint rule that was introduced in [12] as the first time stepping algorithm for non-smooth dynamic systems. This discretization scheme has been used for the numerical integration of the woodpecker's equation of motion to obtain the results shown in Section 4. In Section 6 we finally show how the linear complementarity problem has to be formulated for planar Coulomb contacts by using the discretized equations of Section 5. This procedure has been taken from [8] and has been adapted to account for impacts.

2. Basic Set-Valued Elements

A *linear complementarity problem* (LCP) is a problem of the following form [3, 15]: For given $\mathbf{A} \in \mathbb{R}^{n,n}$ and $\mathbf{b} \in \mathbb{R}^n$, find $\mathbf{x} \in \mathbb{R}^n$ and $\mathbf{y} \in \mathbb{R}^n$ such that the linear equation $\mathbf{y} = \mathbf{A}\mathbf{x} + \mathbf{b}$ holds together with the complementarity conditions $y_i \geq 0$, $x_i \geq 0$, $y_i\, x_i = 0$ for $i = 1, \ldots, n$. The latter conditions are often written in the form $\mathbf{y} \succeq 0$, $\mathbf{x} \succeq 0$, $\mathbf{y}^{\mathsf{T}}\mathbf{x} = 0$ or, equivalently, as $0 \preceq \mathbf{y} \perp \mathbf{x} \succeq 0$.

It is convenient to introduce a maximal monotone set-valued map Upr defined on $\mathbb{R}^+$, which we call the *unilateral primitive*, and which is the most important

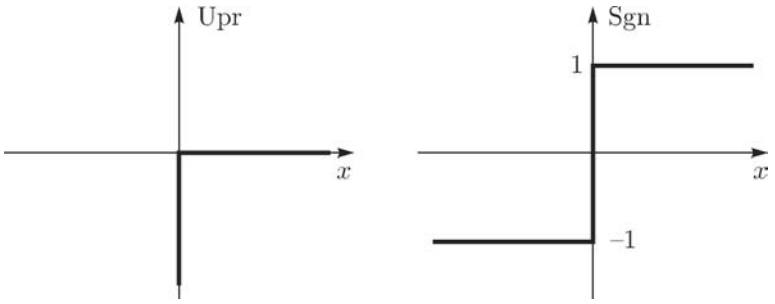

Figure 1. The maps $x \to \mathrm{Upr}(x)$ and $x \to \mathrm{Sgn}\,(x)$.

multifunction related to complementarity,

$$\mathrm{Upr}(x) := \begin{cases} \{0\} & \text{if } x > 0 \\ (-\infty, 0] & \text{if } x = 0 \end{cases}. \tag{1}$$

The graph of this map is depicted in the left part of Figure 1. Apparently, we are now able to express each complementarity condition of the LCP by one inclusion, since

$$-y \in \mathrm{Upr}(x) \;\Leftrightarrow\; y \geq 0, \;\; x \geq 0, \;\; xy = 0. \tag{2}$$

Unilateral primitives are used in mechanics on displacement level and on velocity level to model unilateral geometric and kinematic constraints, such as free plays with stops, sprag clutches and the like. The associated set-valued force laws are conveniently stated as inclusions in the form (2).

A second maximal monotone set-valued map, frequently met in complementarity systems, is the filled-in *relay function* $\mathrm{Sgn}\,(x)$, defined by

$$\mathrm{Sgn}\,(x) := \begin{matrix} \{+1\} & \text{if } x > 0 \\ [-1, +1] & \text{if } x = 0\,, \\ \{-1\} & \text{if } x < 0 \end{matrix} \tag{3}$$

see Figure 1 for the graph. Note the difference at $x = 0$ to the classical sgn-function, which is defined as $\mathrm{sgn}\,(x = 0) = 0$. In mechanics, relay functions on velocity level are used to model any kind of dry friction. On displacement level, they describe the behavior of pre-stressed springs. The relay function (3) can be represented by two unilateral primitives as indicated in Figure 2, which yields in terms of inclusions

$$-y \in \mathrm{Sgn}\,(x) \quad \Leftrightarrow \quad \exists\, x_R,\, x_L \text{ such that } \begin{cases} -y \in +\mathrm{Upr}(x_R) + 1 \\ -y \in -\mathrm{Upr}(x_L) - 1 \\ x = x_R - x_L \end{cases}. \tag{4}$$

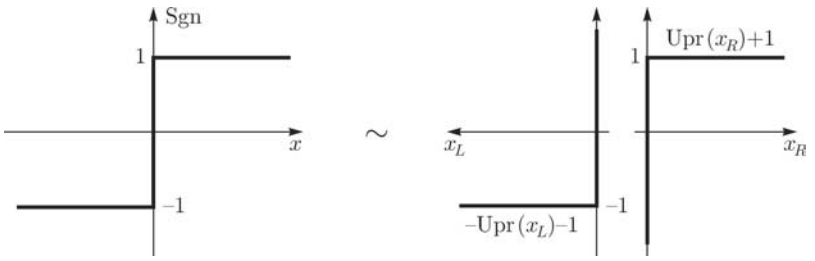

Figure 2. Decomposition of Sgn into Upr's.

More details on this decomposition may be found in [8] together with various applications of even more complex set-valued interaction laws and their representations via unilateral primitives and inclusions. By using Equation (2), we may finally express Equation (4) in terms of complementarities,

$$-y \in \operatorname{Sgn}(x) \Leftrightarrow \exists\, x_R,\ x_L \text{ s.t. } \begin{cases} 1+y \geq 0,\ x_R \geq 0,\ (1+y)\,x_R = 0 \\ 1-y \geq 0,\ x_L \geq 0,\ (1-y)\,x_L = 0\ . \\ x = x_R - x_L \end{cases} \quad (5)$$

This representation has to be used when a problem involving Sgn-multifunctions is formulated as an LCP in standard form.

3. Mechanical Systems with Planar Coulomb Friction

The most suitable way to express the Newton–Euler equations for non-smooth dynamics is in terms of an equality of measures as introduced in [12]. In addition to non-smooth impact-free motion, this formulation covers even impulsive behavior and should be considered as the starting point of any such problem in dynamics.

The following notation is used: $I := [t_A, t_E]$ denotes a compact time interval on which the motion of the system is of interest. Time is denoted by t, and the Lebesgue measure on $\mathbb{R}$ by $\mathrm{d}t$. We investigate the dynamics of a mechanical system on an f-dimensional configuration manifold with frictional boundaries. The set of local coordinates in use is denoted by $\mathbf{q} \in \mathbb{R}^f$, and the associated velocities by $\mathbf{u} \in \mathbb{R}^f$. As functions of time, the velocities $\mathbf{u}$: $[t_A, t_E] \to \mathbb{R}^f$ are assumed to be of bounded variation with differential measure $\mathrm{d}\mathbf{u}$, leading to displacements $\mathbf{q}(t) = \mathbf{q}(t_A) + \int_{t_A}^{t} \mathbf{u}(\tau)\,\mathrm{d}\tau$ that are absolutely continuous on I with $\dot{\mathbf{q}} = \mathbf{u}$ almost everywhere. We further denote the right and left limit of $\mathbf{u}(t)$ at t by $\mathbf{u}^+(t)$ and $\mathbf{u}^-(t)$, respectively, which might be different from each other in the case of an impact. For a thorough treatment of bounded variation functions, absolute continuity and measures we refer in particular to the article [13], or to any advanced text book on integration theory, such as [21] or [5]. The measure equality for such a dynamic

system reads as

$$\mathbf{M}\,\mathrm{d}\mathbf{u} - \mathbf{h}\,\mathrm{d}t - \mathrm{d}\mathbf{R} = 0, \tag{6}$$

where $\mathbf{M}(\mathbf{q}, t)$ is the symmetric and positive definite mass matrix of the system, $\mathbf{h}(\mathbf{q}, \mathbf{u}, t)$ the f-tuple of the gyroscopic accelerations (Christoffel symbols) together with all classical finite-valued generalized forces, and $\mathrm{d}\mathbf{R}$ the force measure of possibly atomic impact impulsions, in our case containing the contact forces. The terms $\mathbf{M}$ and $\mathbf{h}$ can be derived, for example, by taking $\mathbf{q}$ as a set of classical generalized coordinates of the system and evaluating Lagrange's equations of second kind or the associated virtual work expressions. The resulting classical second order equation $\mathbf{M}(\mathbf{q}, t)\,\ddot{\mathbf{q}} - \mathbf{h}(\mathbf{q}, \dot{\mathbf{q}}, t) = 0$ would then describe the same system as above, but without any contacts and any contact forces.

We assume a total of n frictional unilateral constraints in the system, which are represented by n inequalities

$$g_{Ni}(\mathbf{q}, t) \geq 0, \quad i = 1, \ldots, n. \tag{7}$$

The quantities g_{Ni} are the gap functions of the frictional contacts. They are formulated such that $g_{Ni} > 0$ indicates an open contact with an Euclidean distance of the contact points given by the value of g_{Ni}, $g_{Ni} = 0$ corresponds to a closed contact, and $g_{Ni} < 0$ indicates forbidden overlapping or interpenetration. A detailed description on how to define these inequalities in a multibody system may be found in [20]. We further introduce the set of active contacts

$$\mathcal{H}(t) = \big\{ i \mid g_{Ni}(\mathbf{q}(t), t) = 0 \big\}, \tag{8}$$

which singles out the contacts at which contact forces may occur. The force measure $\mathrm{d}\mathbf{R}$ in Equation (6) is therefore at most composed of the normal and tangential contact forces of the individuals $i \in \mathcal{H}$ and may be written as

$$\mathrm{d}\mathbf{R} = \sum_{i \in \mathcal{H}} \mathbf{w}_{Ni}\,\mathrm{d}\Lambda_{Ni} + \mathbf{w}_{Ti}\,\mathrm{d}\Lambda_{Ti}. \tag{9}$$

In this expression, $(\mathbf{w}_{Ni}, \mathbf{w}_{Ti})(\mathbf{q}, t)$ are the generalized normal and tangential force directions, and $(\mathrm{d}\Lambda_{Ni}, \mathrm{d}\Lambda_{Ti})$ the associated scalar normal and tangential contact impulse measures of contact i. Note that integration over a singleton t gives the scalar impulsive contact forces, $\int_{\{t\}} (\mathrm{d}\Lambda_{Ni}, \mathrm{d}\Lambda_{Ti}) = (\Lambda_{Ni}(t), \Lambda_{Ti}(t))$. In case of impact-free motion, one obtains from the same expression that $(\mathrm{d}\Lambda_{Ni}, \mathrm{d}\Lambda_{Ti}) = (\dot{\Lambda}_{Ni}, \dot{\Lambda}_{Ti})\,\mathrm{d}t$ with $\dot{\Lambda}_{Ni}$ the normal and $\dot{\Lambda}_{Ti}$ the tangential scalar contact force.

The system's dynamics is not yet completely determined by Equations (6–9), because we still have to specify force laws that relate the contact impulse measures

$(\mathrm{d}\Lambda_{Ni},\ \mathrm{d}\Lambda_{Ti})$ to the system's kinematic state $(\mathbf{q},\ \mathbf{u})$. To do so, we first introduce the normal and tangential relative velocities in the contacts,

$$\gamma_{Ni} = \mathbf{w}_{Ni}^{\mathsf{T}}\,\mathbf{u} + \hat{w}_{Ni}, \qquad \gamma_{Ti} = \mathbf{w}_{Ti}^{\mathsf{T}}\,\mathbf{u} + \hat{w}_{Ti} \tag{10}$$

with $(\mathbf{w}_{Ni},\ \mathbf{w}_{Ti})(\mathbf{q}, t)$ as in Equation (9) and $(\hat{w}_{Ni},\ \hat{w}_{Ti})(\mathbf{q}, t) \neq (0,\ 0)$ only for rheonomic systems, see e.g. [20] on how to obtain these terms. We choose for the normal direction of each contact a unilateral version of Newton's impact law with local restitution coefficient $\varepsilon_{Ni} \in [0,\ 1]$, and for the tangential direction a Coulomb type frictional law with friction coefficient μ_i that is complemented by a tangential restitution behavior $\varepsilon_{Ti} \in [0,\ 1]$. We define

$$\xi_{Ni} := \gamma_{Ni}^{+} + \varepsilon_{Ni}\,\gamma_{Ni}^{-}, \qquad \xi_{Ti} := \gamma_{Ti}^{+} + \varepsilon_{Ti}\,\gamma_{Ti}^{-}, \tag{11}$$

where $(\gamma_{Ni}^{\pm},\ \gamma_{Ti}^{\pm}) := (\gamma_{Ni},\ \gamma_{Ti})(\mathbf{u}^{\pm})$, and pose the normal and tangential impact laws as

$$-\mathrm{d}\Lambda_{Ni} \in \mathrm{Upr}(\xi_{Ni}), \qquad -\mathrm{d}\Lambda_{Ti} \in \mu_i\,\mathrm{d}\Lambda_{Ni}\,\mathrm{Sgn}\,(\xi_{Ti}). \tag{12}$$

With Equations (6–12) we have now obtained a complete description of the dynamics of the system, including both, impacts and impact-free motion.

Note that the impact laws (12) are actually impact-contact laws, because they hold for both, impacts and impact-free motion: In the first case, $(\mathrm{d}\Lambda_{Ni},\ \mathrm{d}\Lambda_{Ti})$ in Equation (12) has just to be replaced by the corresponding impulsive forces $(\Lambda_{Ni},\ \Lambda_{Ti})\,(t)$ when integration over $\{t\}$ has been performed. For the second case, assume a time interval without impacts, i.e. a time interval in which the velocities are continuous $\mathbf{u}^{+} = \mathbf{u}^{-} = \mathbf{u}$ and the forces are non-impulsive $(\mathrm{d}\Lambda_{Ni},\ \mathrm{d}\Lambda_{Ti}) = (\dot{\Lambda}_{Ni},\ \dot{\Lambda}_{Ti})\,\mathrm{d}t$. Under these assumptions, Equations (11) becomes

$$\xi_{Ni} = (1 + \varepsilon_{Ni})\,\gamma_{Ni}, \qquad \xi_{Ti} = (1 + \varepsilon_{Ti})\,\gamma_{Ti},$$

which causes Equation (12) to be

$$-\dot{\Lambda}_{Ni}\,\mathrm{d}t \in \mathrm{Upr}((1 + \varepsilon_{Ni})\,\gamma_{Ni}), \qquad -\dot{\Lambda}_{Ti}\,\mathrm{d}t \in \mu_i\,\dot{\Lambda}_{Ni}\,\mathrm{d}t\,\mathrm{Sgn}\,((1 + \varepsilon_{Ti})\,\gamma_{Ti}).$$

With non-negative values of the restitution coefficients, $\varepsilon_{Ni} \geq 0$ and $\varepsilon_{Ti} \geq 0$, and after "crossing out" $\mathrm{d}t$ from both inclusions, one obtains

$$-\dot{\Lambda}_{Ni} \in \mathrm{Upr}(\gamma_{Ni}), \qquad -\dot{\Lambda}_{Ti} \in \mu_i\,\dot{\Lambda}_{Ni}\,\mathrm{Sgn}\,(\gamma_{Ti}),$$

which are the force laws for impact-free motion of unilaterally constrained contacts with Coulomb friction [8, 20].

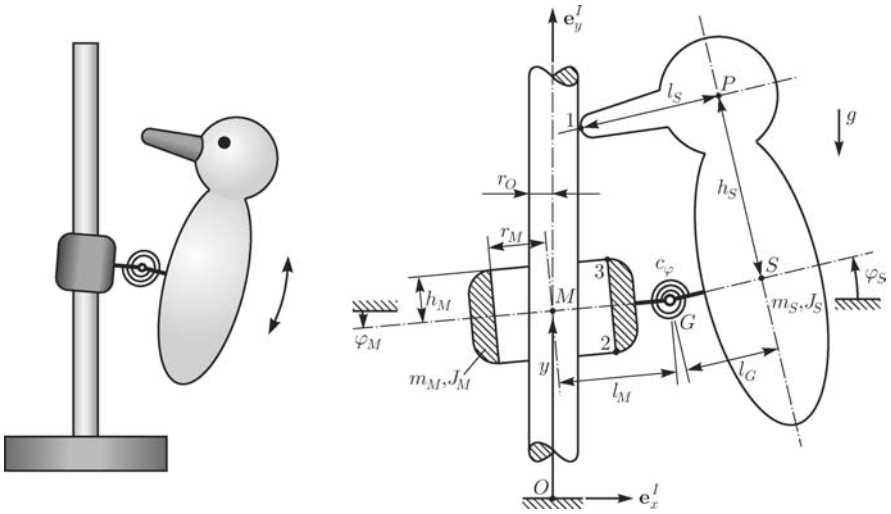

Figure 3. Woodpecker toy and mechanical model.

4. The Woodpecker Toy

A woodpecker hammering down a pole is a typical low-dimensional system combining unilateral constraints, impacts, Coulomb friction and jamming. The woodpecker toy (Figure 3) consists of a pole, a sleeve with a hole that is slightly larger than the diameter of the pole, a spring and the woodpecker. In operation, the woodpecker moves down the pole performing some kind of pitching motion, which is controlled by the sleeve. This mechanism of self-excitation may roughly be explained as follows: Gravitation acts as an energy source. This energy is transmitted to the woodpecker and results in a vertical downward motion of the entire system. The woodpecker itself oscillates up and down. This oscillation interacts via the spring with the sleeve. It gains its energy from the downwards motion by turning the sleeve and switching on and off a frictional contact jamming of the sleeve at the pole. This mechanism ends up in a stable limit cycle with an energetic balance of the kinetic energy, gained per cycle by the falling height, and the dissipated energy due to the frictional contacts.

A planar model of the woodpecker toy is also shown in Figure 3. It consists of three rigid bodies: The woodpecker (center of mass S, mass m_S, moment of inertia J_S), the sleeve (center of mass M, mass m_M, moment of inertia J_M), and the pole that is fixed to the environment. The woodpecker and the sleeve are connected by a revolute joint with angular stiffness c_φ and are both under the influence of gravity g. We equipped the system with three degrees of freedom that are the angular displacement φ_S of the woodpecker, and the angular and vertical displacements φ_M and y of the sleeve. Lateral deviations of the sleeve are small and thus not considered in the model. We further denote the angular velocity of the woodpecker

by ω_S, and the angular and vertical velocities of the sleeve by ω_M and v. The generalized coordinates $\mathbf{q}$ and associated velocities $\mathbf{u}$ may thus be stated as

$$\mathbf{q} = \begin{pmatrix} y \\ \varphi_M \\ \varphi_S \end{pmatrix}, \quad \mathbf{u} = \begin{pmatrix} v \\ \omega_M \\ \omega_S \end{pmatrix} \qquad \text{with } \dot{\mathbf{q}} = \mathbf{u} \text{ almost everywhere.} \tag{13}$$

The special geometrical design of the toy led us to assume only small deviations in the displacements during operation. Thus we set up the dynamic Equations (6–10) based on a linearized kinematics. The mass matrix $\mathbf{M}$ and the vector $\mathbf{h}$ in Equation (6),

$$\begin{aligned} \mathbf{M} &= \begin{pmatrix} m_S + m_M & m_S\, l_M & m_S\, l_G \\ m_S\, l_M & J_M + m_S\, l_M^2 & m_S\, l_M\, l_G \\ m_S\, l_G & m_S\, l_M\, l_G & J_S + m_S\, l_G^2 \end{pmatrix}, \\ \mathbf{h} &= \begin{pmatrix} -(m_S + m_M)g \\ -c_\varphi(\varphi_M - \varphi_S) - m_S\, l_M\, g \\ -c_\varphi(\varphi_S - \varphi_M) - m_S\, l_G\, g \end{pmatrix}, \end{aligned} \tag{14}$$

follow in a straightforward manner from the kinetic and potential energy of the system by working out Lagrange's equations of second kind.

Altogether we take into account three different frictional contacts: Contact 1 is between the beak of the woodpecker and the pole. This contact constraint is not necessary for the woodpecker to work, but as beak impacts have been observed in reality, we want them to be included in our model. The more important contacts are between the sleeve and the pole: The diameter of the hole in the sleeve is slightly larger than the diameter of the pole. Due to the resulting clearance, the lower or upper edge of the sleeve may come into contact with the pole. This is modeled by the unilateral constraints 2 and 3. In particular, the lower sleeve contact 2 is most essential for the jamming mechanism to be switched on and off. The three gap functions (7) follow now directly from Figure 5,

$$\begin{aligned} g_{N1} &= (l_M + l_G - l_S - r_O) - h_S\, \varphi_S, \\ g_{N2} &= (r_M - r_O) + h_M\, \varphi_M, \\ g_{N3} &= (r_M - r_O) - h_M\, \varphi_M. \end{aligned} \tag{15}$$

The relative velocities (10) in the normal directions γ_{Ni} are directly obtained by differentiating the gap functions (15) with respect to time. In the tangential directions, the γ_{Ti} follow easily from Figure 5. The associated $\mathbf{w}$ vectors and $\hat{w}$ scalars

that are also needed to set up the force measure d**R** in Equation (9) are

$$\begin{aligned}
\mathbf{w}_{N1} &= \begin{pmatrix} 0 \\ 0 \\ -h_S \end{pmatrix}, \quad \mathbf{w}_{T1} = \begin{pmatrix} 1 \\ l_M \\ l_G - l_S \end{pmatrix}, \quad \hat{w}_{N1} = \hat{w}_{T1} = 0, \\
\mathbf{w}_{N2} &= \begin{pmatrix} 0 \\ h_M \\ 0 \end{pmatrix}, \quad \mathbf{w}_{T2} = \begin{pmatrix} 1 \\ r_M \\ 0 \end{pmatrix}, \quad \hat{w}_{N2} = \hat{w}_{T2} = 0, \\
\mathbf{w}_{N3} &= \begin{pmatrix} 0 \\ -h_M \\ 0 \end{pmatrix}, \quad \mathbf{w}_{T3} = \begin{pmatrix} 1 \\ r_M \\ 0 \end{pmatrix}, \quad \hat{w}_{N3} = \hat{w}_{T3} = 0.
\end{aligned} \tag{16}$$

Numerical integration of the system has been performed by applying the time stepping method described in the next section. The parameters used together with the initial conditions are summarized in Table I. The numerical results in Figures 4–6 obtained by this method have been confirmed by at least three independent calculations based on different numerical schemes. Among them was an event-driven evaluation which is published in [11], and which is complemented by a deep discussion of the bifurcation behavior of the system.

For the woodpecker example, the maximal dimension of the associated linear complementarity problems is 6. This dimension results from at most two contacts that can be closed at the same time, with three equations each. This is due to the special woodpecker kinematics which excludes a simultaneous contact of the upper and lower edge of the sleeve. An LCP of dimension 6 requires $2^6 = 64$ different cases to be checked for consistency. Not all of them are physically admissible because of one slack variable per contact that has to be introduced for technical reasons. However, 16 different physical states are still possible. They result from any combination of four contact states of the contacts in the LCP, i.e. sticking, separation, and two different directions of sliding. If a structured inequality approach like an LCP formulation is avoided, and the system is classically treated by a combinatorial trial and error method, these 16 states have to be evaluated "by hand". This requires already a certain effort, but becomes impracticable for problems of higher dimensions with some hundreds or thousands of contacts.

5. Time Discretization

One of the main topics of present research in non-smooth dynamics is the development of reliable numerical integration algorithms for measure differential inclusions from both the practical and the theoretical point of view. Much effort is put today in the further development of the so-called time-stepping methods, of which the first has been proposed as the midpoint rule in [12]. Time-stepping methods are

Table I. Parameters and initial conditions.

Geometry	Radius of pole	$r_O = 0.0025\,\mathrm{m}$
	Inner radius of sleeve	$r_M = 0.0031\,\mathrm{m}$
	$\frac{1}{2}$ Height of sleeve	$h_M = 0.0058\,\mathrm{m}$
	Distance M–G	$l_M = 0.010\,\mathrm{m}$
	Distance G–S	$l_G = 0.015\,\mathrm{m}$
	Distance S–P	$h_S = 0.02\,\mathrm{m}$
	Length of beak P–1	$l_S = 0.0201\,\mathrm{m}$
Inertias	Mass, sleeve	$m_M = 0.0003\,\mathrm{kg}$
	Mass, woodpecker	$m_S = 0.0045\,\mathrm{kg}$
	Moment of inertia, sleeve	$J_M = 5.0 \cdot 10^{-9}\,\mathrm{kg\,m^2}$
	Moment of inertia, woodpecker	$J_S = 7.0 \cdot 10^{-7}\,\mathrm{kg\,m^2}$
Force elements	Angular stiffness, spring	$c_\varphi = 0.0056\,\mathrm{Nm\,rad^{-1}}$
	Gravity	$g = 9.81\,\mathrm{m\,s^{-2}}$
Contact parameters	Normal restitution	$\varepsilon_{N1} = 0.5$
		$\varepsilon_{N2,3} = 0$
	Tangential restitution	$\varepsilon_{T1,2,3} = 0$
	Friction coefficients	$\mu_{1,2,3} = 0.3$
Initial conditions	Sleeve, displacement	$y(0) = 0\,\mathrm{m}$
	Sleeve, angle	$\varphi_M(0) = -0.1036\,\mathrm{rad}$
	Woodpecker, angle	$\varphi_S(0) = -0.2788\,\mathrm{rad}$
	Sleeve, velocity	$v(0) = -0.3411\,\mathrm{m\,s^{-1}}$
	Sleeve, angular velocity	$\omega_M(0) = 0\,\mathrm{rad\,s^{-1}}$
	Woodpecker, angular velocity	$\omega_S(0) = -7.4583\,\mathrm{rad\,s^{-1}}$

difference schemes including fully the complementarity conditions and the impact laws, by allowing a simultaneous treatment of impulsive and non-impulsive forces together with all inequalities involved.

In this section we review the original midpoint rule [12] that has been used for the numerical evaluation of the woodpecker toy. Generally, to perform numerical integration of a system (6–12) with respect to time, one has to address the following problem: For given initial time t^A and known initial displacements $\mathbf{q}^A := \mathbf{q}(t^A) \in \mathbb{R}^f$ and velocities $\mathbf{u}^A := \mathbf{u}(t^A) \in \mathbb{R}^f$, find approximations of the displacements $\mathbf{q}^E := \mathbf{q}(t^E) \in \mathbb{R}^f$ and velocities $\mathbf{u}^E := \mathbf{u}(t^E) \in \mathbb{R}^f$ at the end t^E of a chosen time interval $[t^A,\ t^E]$. To apply the midpoint rule, the following steps have to be performed, see [14] for many helpful additional comments:

1. Choose a time step Δt and compute the midpoint $t^M := t^A + \frac{1}{2}\Delta t$ and the endpoint $t^E := t^A + \Delta t$ of the time interval
2. Compute the midpoint displacements $\mathbf{q}^M := \mathbf{q}^A + \frac{1}{2}\Delta t \cdot \mathbf{u}^A \in \mathbb{R}^f$

3. Matrix calculations:

   (a) Compute $\mathbf{M}(\mathbf{q}^M, t^M) \in \mathbb{R}^{f,f}$ and $\mathbf{h}(\mathbf{q}^M, \mathbf{u}^A, t^M) \in \mathbb{R}^f$
   (b) For $i = 1, \ldots, n$ set up the index set $\mathcal{H} := \{ i \mid g_{Ni}(\mathbf{q}^M, t^M) \leq 0 \}$ with k elements $i_1, \ldots, i_k$ $(0 \leq k \leq n)$
   (c) For every $i \in \mathcal{H}$ compute $\mathbf{w}_{Ni}(\mathbf{q}^M, t^M) \in \mathbb{R}^f$ and $\hat{w}_{Ni}(\mathbf{q}^M, t^M) \in \mathbb{R}$, as well as $\mathbf{w}_{Ti}(\mathbf{q}^M, t^M) \in \mathbb{R}^f$ and $\hat{w}_{Ti}(\mathbf{q}^M, t^M) \in \mathbb{R}$

4. Computation of $\mathbf{u}^E$: In this step, equations (6), (9), (10), (11) and inclusions (12) have to be solved: Find $\mathbf{u}^E$ such that for every $i \in \mathcal{H}$

$$
\begin{aligned}
&(6,9): \quad \mathbf{M}(\mathbf{u}^E - \mathbf{u}^A) - \mathbf{h}\,\Delta t - \sum_{i \in \mathcal{H}} (\mathbf{w}_{Ni}\,\Lambda_{Ni} + \mathbf{w}_{Ti}\,\Lambda_{Ti}) = 0 \\
&(10): \quad \gamma_{Ni}^E = \mathbf{w}_{Ni}^{\mathsf{T}}\,\mathbf{u}^E + \hat{w}_{Ni} \qquad \gamma_{Ti}^E = \mathbf{w}_{Ti}^{\mathsf{T}}\,\mathbf{u}^E + \hat{w}_{Ti} \\
&(10): \quad \gamma_{Ni}^A = \mathbf{w}_{Ni}^{\mathsf{T}}\,\mathbf{u}^A + \hat{w}_{Ni} \qquad \gamma_{Ti}^A = \mathbf{w}_{Ti}^{\mathsf{T}}\,\mathbf{u}^A + \hat{w}_{Ti} \\
&(11): \quad \xi_{Ni} = \gamma_{Ni}^E + \varepsilon_{Ni}\,\gamma_{Ni}^A \qquad \xi_{Ti} = \gamma_{Ti}^E + \varepsilon_{Ti}\,\gamma_{Ti}^A \\
&(12): \quad -\Lambda_{Ni} \in \mathrm{Upr}(\xi_{Ni}) \qquad -\Lambda_{Ti} \in \mu_i\,\Lambda_{Ni}\,\mathrm{Sgn}(\xi_{Ti})
\end{aligned}
\tag{17}
$$

5. Computation of $\mathbf{q}^E := \mathbf{q}^M + \frac{1}{2}\Delta t \cdot \mathbf{u}^E \in \mathbb{R}^f$

More advanced discretization schemes may be found in the literature, such as the powerful Θ-method in [9], an algorithm based on displacements with proven convergence [18, 19], or several other well-developed codes described in [22, 23, 2].

The inequality problem (17) can be solved numerically by many different methods. For example, a Gauß–Seidel iteration is used in [14] in which the contacts are solved cyclically independent of each other. Another iterative algorithm, introduced in [16], splits the Coulomb contact problems into one overall normal and one overall tangential subproblem which are then alternately solved by optimization techniques until convergence. The associated variational formulations and convex minimization problems on acceleration level for multibody systems can be found in [7] and [8]. A powerful way to directly solve (17) via a non-smooth Newton method is the Augmented Lagrangian approach which was introduced into mechanics by [1], see e.g. [10] for a review and [4] for the kinematical and mechanical formulation of the contact laws. Another possibility is to reformulate (17) as a complementarity problem in standard form and to invoke an appropriate solver. Such formulations may be found, among many others, in [22] and [17] along with proofs on existence and uniqueness of solutions. Depending on the choice of the numerical discretization scheme, the resulting complementarity problem will be linear as in our case, or nonlinear. Solution methods for nonlinear complementarity problems based on NCP-functions and a semi-smooth Newton algorithm are presented, for example, in [6].

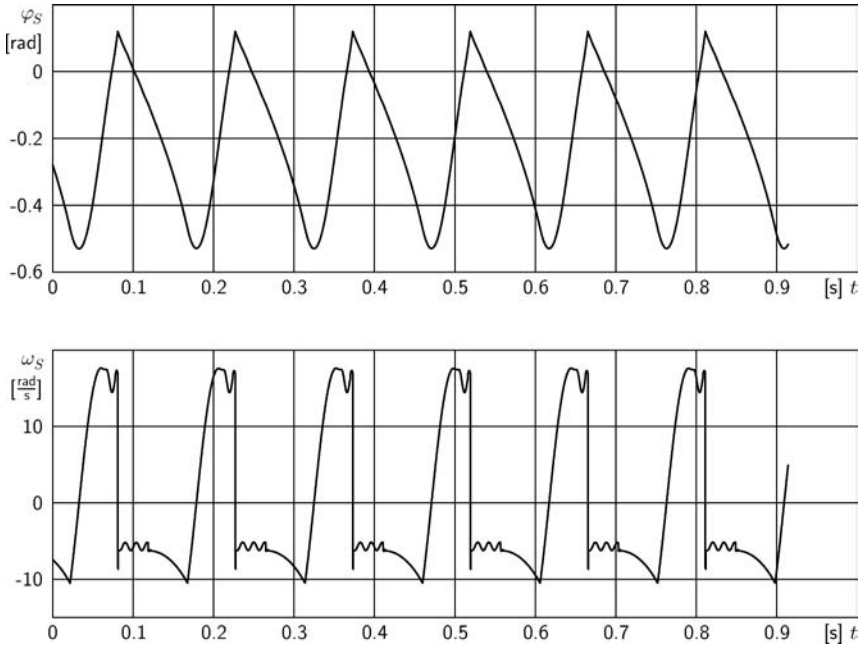

Figure 4. Time history of the woodpecker's angular displacement and velocity.

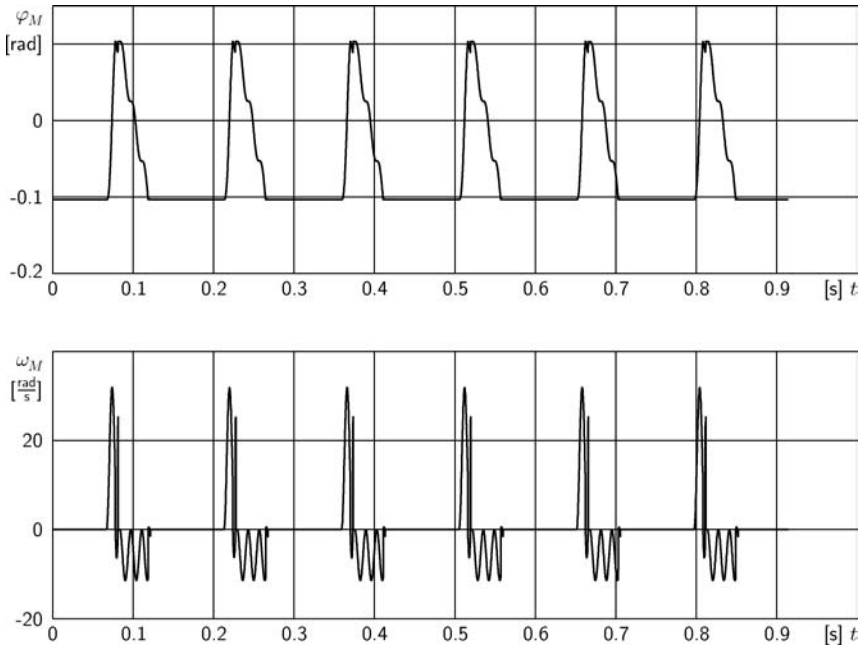

Figure 5. Time history of the sleeve's angular displacement and velocity.

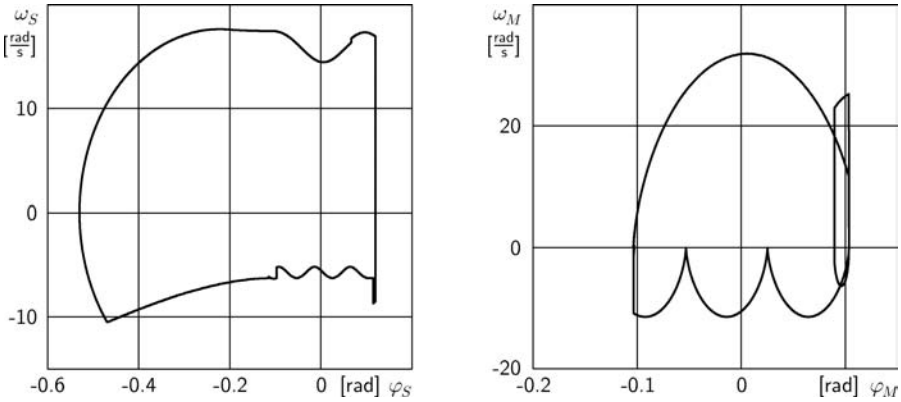

Figure 6. Limit cycle in the phase space.

In this paper, we choose to formulate (17) as a linear complementarity problem in standard form, which will be done in the next section, and to invoke finally an appropriate LCP solver, based on the algorithms found in [3] and [15].

6. Setting up the LCP

The purpose of this section is to derive an LCP formulation of the inequality problem (17). This step is nontrivial and tricky, and *must not be underestimated*. The main difficulty stems from the Sgn -functions that have to be decomposed into Upr's to achieve the desired complementarity formulation.

Many different approaches can be found in literature on how to perform this decomposition. Slack variables are introduced in various ways to express the relay function by complementarity conditions. Most of them, however, have serious disadvantages with respect to the dimension or the structure of the resulting LCP. Possible relations to optimization theory may easily be disguised when slack variables are introduced in an ad hoc manner. Other problems are that additional solutions, that means solutions that are *not* contained in the original problem and thus *contradict the original problem*, might be generated when too many slack variables are introduced without the necessary care, or that unnecessary matrix inversions have to be performed. Another attempt that is frequently undertaken and that does *not* solve the problem is to slightly shift the set-valuedness of the sgn-function away from the origin to a neighboring point.

We are convinced that our approach is *the only reasonable* one when an LCP representation in local variables is desired for systems involving relay functions, and that this approach is even general enough to be applied without any modifications for adjoint problems in electrical networks or hydraulics. The steps that we perform

to derive the LCP follow exactly the procedure described in [8] to approximate even spatial friction by friction pyramides. To set up the LCP, rigorous matrix notation is required. We define

$$
\begin{aligned}
\mathbf{W}_N &:= \left(\mathbf{w}_{Ni_1}, \ldots, \mathbf{w}_{Ni_k}\right), & \mathbf{W}_T &:= \left(\mathbf{w}_{Ti_1}, \ldots, \mathbf{w}_{Ti_k}\right) \in \mathbb{R}^{f,k} \\
\hat{\mathbf{w}}_N &:= \left(\hat{w}_{Ni_1}, \ldots, \hat{w}_{Ni_k}\right)^{\mathsf{T}}, & \hat{\mathbf{w}}_T &:= \left(\hat{w}_{Ti_1}, \ldots, \hat{w}_{Ti_k}\right)^{\mathsf{T}} \in \mathbb{R}^{k} \\
\boldsymbol{\Lambda}_N &:= \left(\Lambda_{Ni_1}, \ldots, \Lambda_{Ni_k}\right)^{\mathsf{T}}, & \boldsymbol{\Lambda}_T &:= \left(\Lambda_{Ti_1}, \ldots, \Lambda_{Ti_k}\right)^{\mathsf{T}} \in \mathbb{R}^{k} \\
\boldsymbol{\gamma}_N^E &:= \left(\gamma_{Ni_1}^E, \ldots, \gamma_{Ni_k}^E\right)^{\mathsf{T}}, & \boldsymbol{\gamma}_T^E &:= \left(\gamma_{Ti_1}^E, \ldots, \gamma_{Ti_k}^E\right)^{\mathsf{T}} \in \mathbb{R}^{k} \\
\boldsymbol{\gamma}_N^A &:= \left(\gamma_{Ni_1}^A, \ldots, \gamma_{Ni_k}^A\right)^{\mathsf{T}}, & \boldsymbol{\gamma}_T^A &:= \left(\gamma_{Ti_1}^A, \ldots, \gamma_{Ti_k}^A\right)^{\mathsf{T}} \in \mathbb{R}^{k} \\
\boldsymbol{\xi}_N &:= \left(\xi_{Ni_1}, \ldots, \xi_{Ni_k}\right)^{\mathsf{T}}, & \boldsymbol{\xi}_T &:= \left(\xi_{Ti_1}, \ldots, \xi_{Ti_k}\right)^{\mathsf{T}} \in \mathbb{R}^{k} \\
\boldsymbol{\epsilon}_N &:= \operatorname{diag}\left(\varepsilon_{Ni_1}, \ldots, \varepsilon_{Ni_k}\right), & \boldsymbol{\epsilon}_T &:= \operatorname{diag}\left(\varepsilon_{Ti_1}, \ldots, \varepsilon_{Ti_k}\right) \in \mathbb{R}^{k,k} \\
& & \boldsymbol{\mu} &:= \operatorname{diag}\left(\mu_{i_1}, \ldots, \mu_{i_k}\right) \in \mathbb{R}^{k,k}
\end{aligned}
$$

and rewrite the first four lines in (17) as

$$
\begin{aligned}
&\mathbf{M}\,(\mathbf{u}^E - \mathbf{u}^A) - \mathbf{h}\,\Delta t - \mathbf{W}_N\,\boldsymbol{\Lambda}_N - \mathbf{W}_T\,\boldsymbol{\Lambda}_T = 0, \\
&\boldsymbol{\gamma}_N^E = \mathbf{W}_N^{\mathsf{T}}\,\mathbf{u}^E + \hat{\mathbf{w}}_N\,, \quad \boldsymbol{\gamma}_T^E = \mathbf{W}_T^{\mathsf{T}}\,\mathbf{u}^E + \hat{\mathbf{w}}_T, \\
&\boldsymbol{\gamma}_N^A = \mathbf{W}_N^{\mathsf{T}}\,\mathbf{u}^A + \hat{\mathbf{w}}_N\,, \quad \boldsymbol{\gamma}_T^A = \mathbf{W}_T^{\mathsf{T}}\,\mathbf{u}^A + \hat{\mathbf{w}}_T, \\
&\boldsymbol{\xi}_N = \boldsymbol{\gamma}_N^E + \boldsymbol{\epsilon}_N\,\boldsymbol{\gamma}_N^A, \qquad \boldsymbol{\xi}_T = \boldsymbol{\gamma}_T^E + \boldsymbol{\epsilon}_T\,\boldsymbol{\gamma}_T^A.
\end{aligned}
\tag{18}
$$

The third line in Equation (18) is used to compute $(\boldsymbol{\gamma}_N^A,\ \boldsymbol{\gamma}_T^A)$ from the known velocities $\mathbf{u}^A$ at the left endpoint of the time interval and is thus no longer needed. The unknowns $(\boldsymbol{\gamma}_N^E,\ \boldsymbol{\gamma}_T^E)$ in the fourth line may be immediately eliminated with the help of the second line. This results in the reduced set of equations

$$
\mathbf{M}\,(\mathbf{u}^E - \mathbf{u}^A) - \mathbf{h}\,\Delta t - \mathbf{W}_N\,\boldsymbol{\Lambda}_N - \mathbf{W}_T\,\boldsymbol{\Lambda}_T = 0, \tag{19}
$$

$$
\boldsymbol{\xi}_N = \mathbf{W}_N^{\mathsf{T}}\mathbf{u}^E + \left(\hat{\mathbf{w}}_N + \boldsymbol{\epsilon}_N\,\boldsymbol{\gamma}_N^A\right), \tag{20}
$$

$$
\boldsymbol{\xi}_T = \mathbf{W}_T^{\mathsf{T}}\mathbf{u}^E + \left(\hat{\mathbf{w}}_T + \boldsymbol{\epsilon}_T\,\boldsymbol{\gamma}_T^A\right), \tag{21}
$$

which will be used in the sequel to set up the linear complementarity problem.

We are now going to formulate the inclusions from the last line in (17) as complementarity conditions. For the unilateral primitives we obtain by (2)

$$
\begin{aligned}
&-\Lambda_{Ni} \in \operatorname{Upr}(\xi_{Ni}) \quad (i \in \mathcal{H}) \\
&\quad \Updownarrow \\
&\boldsymbol{\Lambda}_N \succeq 0,\ \boldsymbol{\xi}_N \succeq 0,\ \boldsymbol{\Lambda}_N^{\mathsf{T}}\,\boldsymbol{\xi}_N = 0.
\end{aligned}
\tag{22}
$$

The relay functions have to be decomposed according to (5), but with a modified step height $[-\mu_i \Lambda_{Ni},\ +\mu_i \Lambda_{Ni}]$ which gives

$$
\begin{aligned}
&-\Lambda_{Ti} \in \mu_i\, \Lambda_{Ni}\, \mathrm{Sgn}\,(\xi_{Ti}) \quad (i \in \mathcal{H}) \\
&\quad \Updownarrow \\
&\exists\, \boldsymbol{\xi}_R,\ \boldsymbol{\xi}_L \in \mathbb{R}^k \text{ such that}
\end{aligned}
$$

$$
\begin{cases}
\boldsymbol{\mu\Lambda}_N + \boldsymbol{\Lambda}_T \geq 0,\ \boldsymbol{\xi}_R \geq 0,\ (\boldsymbol{\mu\Lambda}_N + \boldsymbol{\Lambda}_T)^{\mathsf{T}}\, \boldsymbol{\xi}_R = 0 \\
\boldsymbol{\mu\Lambda}_N - \boldsymbol{\Lambda}_T \geq 0,\ \boldsymbol{\xi}_L \geq 0,\ (\boldsymbol{\mu\Lambda}_N - \boldsymbol{\Lambda}_T)^{\mathsf{T}}\, \boldsymbol{\xi}_L = 0\,. \\
\boldsymbol{\xi}_T = \boldsymbol{\xi}_R - \boldsymbol{\xi}_L
\end{cases}
\tag{23}
$$

We further introduce $\boldsymbol{\Lambda}_R, \boldsymbol{\Lambda}_L \in \mathbb{R}^k$ to abbreviate the complementarity conditions in Equation (23). They are defined, together with the last equation in (23), as

$$\boldsymbol{\Lambda}_R := \boldsymbol{\mu\Lambda}_N + \boldsymbol{\Lambda}_T, \tag{24}$$

$$\boldsymbol{\Lambda}_L := \boldsymbol{\mu\Lambda}_N - \boldsymbol{\Lambda}_T, \tag{25}$$

$$\boldsymbol{\xi}_T = \boldsymbol{\xi}_R - \boldsymbol{\xi}_L. \tag{26}$$

The whole set of complementarity conditions (22), (23) therefore reads as

$$0 \preceq \begin{pmatrix} \boldsymbol{\xi}_N \\ \boldsymbol{\xi}_R \\ \boldsymbol{\Lambda}_L \end{pmatrix} \perp \begin{pmatrix} \boldsymbol{\Lambda}_N \\ \boldsymbol{\Lambda}_R \\ \boldsymbol{\xi}_L \end{pmatrix} \succeq 0. \tag{27}$$

Note the special arrangement of $\boldsymbol{\Lambda}_L$ and $\boldsymbol{\xi}_L$ in Equation (27). They *must* be placed in this manner, which has deep roots in optimization theory. Otherwise, one is not able to set up the LCP without additional matrix inversion processes.

By Equation (27) we have already found the final description of the complementarity conditions of our problem, which also defines the vectors of variables that are allowed to be used. In addition, we still have Equations (19–21) and (24–26) with the unknowns $\boldsymbol{\Lambda}_{N,R,L,T}$, $\boldsymbol{\xi}_{N,R,L,T}$ and $\mathbf{u}^E$. The magnitudes $\boldsymbol{\xi}_T$, $\boldsymbol{\Lambda}_T$ and $\mathbf{u}^E$ have to be eliminated from this set of six equations, because they are not contained as variables in Equation (27). In a first step, we use Equation (24) and Equation (26) to remove $\boldsymbol{\Lambda}_T$ and $\boldsymbol{\xi}_T$ from the remaining equations. This yields for Equations (19), (20), (21), (25)

$$\mathbf{M}\,(\mathbf{u}^E - \mathbf{u}^A) - \mathbf{h}\Delta t - (\mathbf{W}_N - \mathbf{W}_T\,\boldsymbol{\mu})\boldsymbol{\Lambda}_N - \mathbf{W}_T\,\boldsymbol{\Lambda}_R = 0, \tag{28}$$

$$\boldsymbol{\xi}_N = \mathbf{W}_N^{\mathsf{T}}\mathbf{u}^E + \left(\hat{\mathbf{w}}_N + \boldsymbol{\epsilon}_N\, \boldsymbol{\gamma}_N^A\right), \tag{29}$$

$$\boldsymbol{\xi}_R = \mathbf{W}_T^{\mathsf{T}}\mathbf{u}^E + \left(\hat{\mathbf{w}}_T + \boldsymbol{\epsilon}_T\, \boldsymbol{\gamma}_T^A\right) + \boldsymbol{\xi}_L, \tag{30}$$

$$\boldsymbol{\Lambda}_L = 2\,\boldsymbol{\mu}\,\boldsymbol{\Lambda}_N - \boldsymbol{\Lambda}_R. \tag{31}$$

In a second step, we solve Equation (28) for $\mathbf{u}^E$, which is always possible due to the regularity of the mass matrix $\mathbf{M}$,

$$\mathbf{u}^E = \mathbf{M}^{-1}(\mathbf{W}_N - \mathbf{W}_T\,\boldsymbol{\mu})\,\boldsymbol{\Lambda}_N + \mathbf{M}^{-1}\mathbf{W}_T\,\boldsymbol{\Lambda}_R + \mathbf{M}^{-1}\mathbf{h}\,\Delta t + \mathbf{u}^A\,, \tag{32}$$

and plug it in Equations (29) and (30). As a result, we obtain (29–31) in matrix notation,

$$\begin{pmatrix} \boldsymbol{\xi}_N \\ \boldsymbol{\xi}_R \\ \boldsymbol{\Lambda}_L \end{pmatrix} = \begin{pmatrix} \mathbf{W}_N^{\mathsf{T}}\mathbf{M}^{-1}(\mathbf{W}_N - \mathbf{W}_T\,\boldsymbol{\mu}) & \mathbf{W}_N^{\mathsf{T}}\mathbf{M}^{-1}\mathbf{W}_T & 0 \\ \mathbf{W}_T^{\mathsf{T}}\mathbf{M}^{-1}(\mathbf{W}_N - \mathbf{W}_T\,\boldsymbol{\mu}) & \mathbf{W}_T^{\mathsf{T}}\mathbf{M}^{-1}\mathbf{W}_T & \mathbf{E} \\ 2\,\boldsymbol{\mu} & -\mathbf{E} & 0 \end{pmatrix} \begin{pmatrix} \boldsymbol{\Lambda}_N \\ \boldsymbol{\Lambda}_R \\ \boldsymbol{\xi}_L \end{pmatrix} + \begin{pmatrix} \mathbf{W}_N^{\mathsf{T}}\mathbf{M}^{-1}\mathbf{h}\,\Delta t + (\mathbf{E} + \boldsymbol{\epsilon}_N)\,\boldsymbol{\gamma}_N^A \\ \mathbf{W}_T^{\mathsf{T}}\mathbf{M}^{-1}\mathbf{h}\,\Delta t + (\mathbf{E} + \boldsymbol{\epsilon}_T)\,\boldsymbol{\gamma}_T^A \\ 0 \end{pmatrix}, \tag{33}$$

where we have used the third line in Equation (18) to express $(\mathbf{W}_N^{\mathsf{T}}\mathbf{u}^A,\ \mathbf{W}_T^{\mathsf{T}}\mathbf{u}^A)$ in terms of $(\boldsymbol{\gamma}_N^A,\ \boldsymbol{\gamma}_T^A)$. Equation (33) together with (27) is now the desired LCP $\mathbf{y} = \mathbf{A}\mathbf{x} + \mathbf{b}$, $0 \preceq \mathbf{y} \perp \mathbf{x} \succeq 0$ of dimension $3k$.

Note the following properties of the LCP (33), (27): For friction that is independent of the normal load Λ_{Ni}, the terms $\mu_i \Lambda_{Ni}$ have to be replaced by constants a_i and move into the vector $\mathbf{b}$ of the LCP. The resulting matrix $\mathbf{A}$ is then bisymmetric, and the LCP states the Kuhn–Tucker conditions of an associated quadratic program with inequality constraints, see [8]. For $\Delta t = 0$, the LCP reduces to the pure impact equations and can be used, for example, for initialization of the velocities. For $\boldsymbol{\gamma}_N^A = \boldsymbol{\gamma}_T^A = 0$, the LCP describes impact-free motion on velocity level, containing still the cases of persisting contact and stiction as well as transitions to sliding or separation, and can be transformed to the acceleration level by the methods shown in [8].

Acknowledgments

Parts of this research was conducted within the European project SICONOS IST-2001-37172 and supported by the Swiss Federal Office for Education and Science (BBW).

References

1. Alart, P. and Curnier, A. A mixed formulation for frictional contact problems prone to Newton like solution methods. *Computer Methods in Applied Mechanics and Engineering* **92**(3), 1991, 353–357.

2. Anitescu, M., Potra, F.A. and Stewart, D.E. Time-stepping for three-dimensional rigid body dynamics. *Computer Methods in Applied Mechanics and Engineering* **177**(3), 1999, 183–197.
3. Cottle, R.W., Pang, J.S. and Stone, R.E. *The Linear Complementarity Problem*, *Computer Science and Scientific Computing*, Academic Press, London, 1992.
4. Curnier, A., He, Q.C. and Klarbring, A. Continuum mechanics modelling of large deformation contact with friction, in *Contact Mechanics*, Raous, M., Jean, M. and Moreau, J.J. (eds.), Plenum Press, New York, 1995, 145–158.
5. Elstrodt, J., *Maß- und Integrationstheorie*, Springer Verlag, Berlin, 1996.
6. Facchinei, F., Fischer, A. and Kanzow, Ch. A semismooth Newton method for variational inequalities: The case of box constraints, in *Complementarity and Variational Problems: State of the Art*, Ferris, M.C. and Pang, J.-S. (eds.), SIAM, Philadelphia, 1997, 76–90.
7. Glocker, Ch. Dynamik von Starrkörpersystemen mit Reibung und Stößen. *VDI-Fortschrittberichte Mechanik/Bruchmechanik*, Reihe 18, Nr. 182, VDI-Verlag, Düsseldorf, 1995.
8. Glocker, Ch. *Set-Valued Force Laws: Dynamics of Non-Smooth Systems*, Springer Verlag, Berlin Heidelberg, 2001.
9. Jean, M. The non-smooth contact dynamics method. *Computer Methods in Applied Mechanics Engineering* **177**, 1999, 235–257.
10. Klarbring, A. Mathematical programming and augmented Lagrangian methods for frictional contact problems. *Proceeding on Contact Mechanics International Symposium*, Lausanne, 1992, 409–422.
11. Leine, R.I., Glocker, Ch. and van Campen, D.H. Nonlinear dynamics and modeling of various wooden toys with impact and friction. *Journal of Vibration and Control* **9**, 2003, 25–78.
12. Moreau, J.J. Unilateral contact and dry friction in finite freedom dynamics, in *Non-Smooth Mechanics and Applications*, Moreau, J.J. and Panagiotopoulos, P.D. (eds.), CISM Courses and Lectures , Vol. 302, Springer Verlag, Wien, 1988, 1–82.
13. Moreau, J.J. Bounded variation in time, in *Topics in Nonsmooth Mechanics* Moreau, J.J. Panagiotopoulos, P.D. and Strang, G. (eds.), Birkhäuser Verlag, Basel, 1988, 1–74.
14. Moreau, J.J., Numerical aspects of the sweeping process. *Computer Methods in Applied Mechanics. Engineering.* **177**, 1999, 329–349.
15. Murty, K.G. *Linear Complementarity, Linear and Nonlinear Programming* (Sigma Series in Applied Mathematics), Vol. 3, Heldermann Verlag, Berlin, 1988.
16. Panagiotopoulos, P.D. A nonlinear programming approach to the unilateral contact-, and friction-boundary value problem in the theory of elasticity. *Ingenieur-Archiv* **44**, 1975, 421–432.
17. Pang, J.S. and Trinkle, J.C. Complementarity formulations and existence of solutions of dynamic multi-rigid-body contact problems with Coulomb friction. *Mathematical Programming* **30**, 1996, 199–226.
18. Paoli, L. and Schatzman, M. A Numerical scheme for impact problems I: The one-dimensional case. *SIAM Journal on Numerical Analysis* **40**(2), 2002, 702–733.
19. Paoli, L. and Schatzman, M. A Numerical scheme for impact problems II: The multidimensional case. *SIAM Journal on Numerical Analysis* **40**(2), 2002, 734–768.
20. Pfeiffer, F. and Glocker, Ch. *Multibody Dynamics with Unilateral Contacts*, Wiley, New York, 1996.
21. Rudin, W. *Real and Complex Analysis*, Tata McGraw-Hill, New Delhi, India, 1981.
22. Stewart, D.E. and Trinkle, J.C. An implicit time-stepping scheme for rigid body dynamics with inelastic collisions and Coulomb friction. *International Journal Numerical Methods Engineering* **39**(15), 1996, 2673–2691.
23. Stewart, D.E. Convergence of a time-stepping scheme for rigid body dynamics and resolution of Painlevé's problem. *Archives of Rational Mechanics and Analysis* **145**, 1998, 215–260.